OPEN ACCESS
Freely Available Online

JOURNAL OF ADVANCED PHARMACEUTICAL SCIENCE AND TECHNOLOGY
ISSN NO: 2328-0182

Research Article

DOI : 10.14302/issn.2328-0182.japst-18-2314

Impact of Consciousness Energy Healing Treatment on the Physicochemical and Thermal Properties of Silver Oxide

Dahryn Trivedi[1], Mahendra Kumar Trivedi[1], Alice Branton[1], Gopal Nayak[1], Snehasis Jana[2,*]

[1]Trivedi Global, Inc., Henderson, USA.

[2]Trivedi Science Research Laboratory Pvt. Ltd., Bhopal, India.

Abstract

Silver oxide (Ag_2O) has the antimicrobial properties, which is insoluble in most of the solvents and sensitive to light. Therefore, this study was performed to evaluate the impact of the Trivedi Effect®-Consciousness Energy Healing Treatment on the physicochemical and thermal properties of Ag_2O powder using modern analytical techniques. The Ag_2O sample was divided into two parts, one part of the sample was considered as the control sample, whereas the other part of the sample received the Biofield Treatment remotely by a renowned Biofield Energy Healer, Dahryn Trivedi and termed as a treated sample. The particle size values were significantly decreased by 26.70% (d_{10}), 20.67% (d_{50}), 18.7% (d_{90}), and 20.57% [D(4,3)], hence, the specific surface area was significantly increased by 32.33% in the treated Ag_2O sample than control sample. PXRD peak intensities and crystallite sizes were significantly altered from -94.93% to 6.18% and -54.19% to 54.89%, respectively, however, the average crystallite size was significantly decreased by 14.66% in the treated sample compared with the control sample. The latent heat of fusion of the treated Ag_2O was significantly decreased by 61.12% compared with the control sample. The total weight loss was significantly increased by 49.34%, hence, the residue amount was 4.05% less in the treated sample than the control sample. These results suggested that the Trivedi Effect® might introduce a new polymorphic form of Ag_2O which would offer better solubility, absorption, and bioavailability of the pharmaceutical formulations and also be advantageous for the pharmaceutical industry when using it as a raw material.

Corresponding author: Snehasis Jana, Trivedi Science Research Laboratory Pvt. Ltd., Bhopal, India. Tel: +91-022-25811234; Email: publication@trivedisrl.com

Keywords: Silver oxide, Consciousness Energy Healing Treatment, The Trivedi Effect®, Particle size, Surface area, PXRD, DSC, TGA/DTG

Received: Aug 22, 2018 **Accepted:** Oct 09, 2018 **Published:** Oct 12, 2018

Editor: Fatma Mady, Minia University Faculty of pharmacy, Egypt.

Introduction

Silver oxide (Ag_2O) is a chemical compound used as a reagent in the laboratory reactions to synthesize other silver compounds (silver chloride, silver nitrate, etc.); as well as in organic chemistry as a mild oxidizing agent (*i.e.,* oxidizes aldehydes to carboxylic acids), and in silver-oxide batteries. It is integrated in fabrics used in surgery since it resists the growth of microorganisms [1-3]. It is also used in concrete and in some swimming pools and spas to protect the water from unwanted microbes. Ag_2O has enhanced antimicrobial properties, hence used as Ag_2O ointment for difficult venous ulcerations, and also an important component of the total wound dressing, which has demonstrated improved microcirculation measurements and healing rate [4]. Ag_2O is very effective in removing carbon dioxide from the humidified air. This characteristic of Ag_2O is extensively used in space missions. Ag_2O nanostructure on porous silicon is used for the optoelectronic application. Ag_2O is also used for the preparation of a pollution control filter for gas sensors, which absorbs airborne poisons and irritants [5, 6]. The Ag_2O is light sensitive, decomposes at lower temperatures (280°C), soluble in acid and alkali, slightly soluble in water, and insoluble in ethanol [1-3].

Physicochemical properties of any objects have great importance for their stability and other application perspectives. The Trivedi Effect®-Biofield Energy Healing Treatment has been scientifically proved to have the significant impact on the physicochemical properties of various living and non-living object(s) [7-9]. The Trivedi Effect® is natural and the only scientifically proven phenomenon in which a person can harness this inherently intelligent energy from the Universe and transmit it anywhere on the planet through the possible mediation of neutrinos [10]. Due to the continuous movement of the electrically charged particles inside the body, a unique para-dimensional electromagnetic field is generated around the body of the living organism known as the "Biofield". Biofield based Energy Healing Therapies have been accepted worldwide and reported with significant positive outcomes against various disease conditions [11]. The National Institutes of Health (NIH) and National Center for Complementary and Alternative Medicine (NCCAM) recommend and included the Energy therapy under the Complementary and Alternative Medicine (CAM) category in addition to other therapies, medicines and practices such as Qi Gong, Tai Chi, yoga, chiropractic/osteopathic manipulation, meditation, massage, acupuncture, acupressure, relaxation techniques, guided imagery, Reiki, hypnotherapy, healing touch, Rolfing structural integration, mindfulness, Ayurvedic medicine, naturopathy, traditional Chinese herbs and medicines, homeopathy, aromatherapy, cranial sacral therapy and applied prayer. The CAM has been accepted by the most of the U.S. population [12, 13]. In the similar way, the Trivedi Effect®-Consciousness Energy Healing Treatment also had shown significant results in different research field, *i.e.,* medical, nutraceutical/pharmaceutical sciences [14-17], microbiology, biotechnology [18-21], organic chemistry [22, 23], agriculture [24, 25], material science [26, 27], etc. Hence, this current study has been designed to evaluate the impact of the Trivedi Effect®-Consciousness Energy Healing Treatment on silver oxide powder using particle size analysis (PSA), powder X-ray diffraction (PXRD), differential scanning calorimetry (DSC), and thermogravimetric analysis (TGA)/ Differential thermogravimetric analysis (DTG).

Materials and Methods

Chemicals and Reagents

The silver oxide (Ag_2O) powder was procured from Sigma Aldrich, India. Remaining chemicals used during the experiments were of analytical grade also purchased in India.

Consciousness Energy Healing Treatment Strategies

The silver oxide powder considered as a test sample was divided into two parts. One part of the silver oxide powder sample was treated with the Trivedi Effect®-Consciousness Energy Healing Treatment remotely under standard laboratory conditions for 3 minutes, known as the Biofield Energy Treated sample. The Biofield Energy Healing Treatment was provided through the healer's unique energy transmission process by the renowned Biofield Energy Healer, Dahryn Trivedi, USA, to one part of the test sample. Consequently, the other part of the test sample was considered as a control or untreated sample (Biofield Energy Treatment was not provided). Further, the control sample was

treated with a "sham" healer for the best comparison with the results of the Biofield Energy Treated silver oxide. However, the sham healer did not have any knowledge about the Biofield Energy Treatment. After that, the Biofield Energy Treated and untreated silver oxide powder samples were kept in sealed conditions and characterized using PSA, PXRD, DSC, and TGA analytical techniques.

Characterization

Particle Size Analysis (PSA)

The particle size analysis of silver oxide powder was performed on Malvern Mastersizer 2000, from the UK, with a detection range between 0.01 µm to 3000 µm using wet method [28, 29]. The sample unit (Hydro MV) was filled with a dispersant medium (sunflower oil) and operated the stirrer at 2500 rpm. The PSA analysis of silver oxide was executed to obtain the average particle size distribution. Where, d(10) µm, d(50) µm, d (90) µm represent particle diameter corresponding to 10%, 50%, and 90% of the cumulative distribution. D (4,3) represents the average mass-volume diameter, and SSA is the specific surface area (m^2/g). The calculations were done by using software Mastersizer Ver. 5.54.

The percent change in particle size (d) for silver oxide powder at below 10% level (d_{10}), 50% level (d_{50}), 90% level (d_{90}), and D(4,3) was calculated using the following equation 1:

$$\%\ \text{change in particle size} = \frac{[d_{Treated} - d_{Control}]}{d_{Control}} \times 100 \quad (1)$$

Where $d_{Control}$ and $d_{Treated}$ are the particle size (µm) for at below 10% level (d_{10}), 50% level (d_{50}), and 90% level (d_{90}) of the control and the Biofield Energy Treated silver oxide samples, respectively.

Percent change in surface area (S) was calculated using the following equation 2:

$$\%\ \text{change in surface area} = \frac{[S_{Treated} - S_{Control}]}{S_{Control}} \times 100 \quad (2)$$

Where $S_{Control}$ and $S_{Treated}$ are the surface area of the control and the Biofield Energy Treated silver oxide, respectively.

Powder X-ray Diffraction (PXRD) Analysis

The PXRD analysis of silver oxide powder was performed with the help of Rigaku MiniFlex-II Desktop X-ray diffractometer (Japan) [30, 31]. The CuKα radiation source tube output voltage used was 30 kV, and tube output current was 15 mA. Scans were performed at room temperature. The average size of individual crystallites of Silver oxide was calculated from PXRD data using the Scherrer's formula (3)

$$G = k\lambda/\beta\cos\theta \quad (3)$$

Where k is the equipment constant (0.94), G is the crystallite size in nm, λ is the radiation wavelength (0.154056 nm for Kα1 emission), β is the full-width at half maximum (FWHM), and θ is the Bragg angle [32].

Percent change in crystallite size (G) of silver oxide was calculated using the following equation 4:

$$\%\ \text{change in crystallite size} = \frac{[G_{Treated} - G_{Control}]}{G_{Control}} \times 100 \quad (4)$$

Where $G_{Control}$ and $G_{Treated}$ are the crystallite size of the control and the Biofield Energy Treated silver oxide samples, respectively.

Differential Scanning Calorimetry (DSC)

The DSC analysis of silver oxide was performed with the help of DSC Q200, TA instruments. The sample of ~0.5-2 mg was loaded to the aluminium sample pan at a heating rate of 10ºC/min from 30°C to 350°C [28, 29]. The % change in melting point (T) was calculated using the following equation 5:

$$\%\ \text{change in melting point} = \frac{[T_{Treated} - T_{Control}]}{T_{Control}} \times 100 \quad (5)$$

Where $T_{Control}$ and $T_{Treated}$ are the melting point of the control and the Biofield Energy Treated silver oxide samples, respectively.

Percent change in the latent heat of fusion (ΔH) was calculated using following equation 6:

$$\%\ \text{change in latent heat of fusion} = \frac{[\Delta H_{Treated} - \Delta H_{Control}]}{\Delta H_{Control}} \times 100 \quad (6)$$

Where $\Delta H_{Control}$ and $\Delta H_{Treated}$ are the latent heat of fusion of the control and the Biofield Energy Treated silver oxide samples, respectively.

Thermal Gravimetric Analysis (TGA) / Differential Thermogravimetric analysis (DTG)

TGA/DTG thermograms of silver oxide were obtained with the help of TGA Q50 TA instruments. The sample of ~3-7 mg was loaded to the platinum crucible

at a heating rate of 10ºC/min from 25°C to 1000°C with the recent literature [28, 29]. The % change in weight loss (W) was calculated using the following equation 7:

$$\% \text{ change in weight loss} = \frac{[W_{Treated} - W_{Control}]}{W_{Control}} \times 100 \quad (7)$$

Where $W_{Control}$ and $W_{Treated}$ are the weight loss of the control and the Biofield Energy Treated silver oxide, respectively.

The % change in maximum thermal degradation temperature (T_{max}) (M) was calculated using the following equation 8:

$$\% \text{ change in Tmax (M)} = \frac{[M_{Treated} - M_{Control}]}{M_{Control}} \times 100 \quad (8)$$

Where $M_{Control}$ and $M_{Treated}$ are the T_{max} values of the control and the Biofield Energy Treated silver oxide, respectively.

Results and Discussion

Particle Size Analysis (PSA)

The particle size and surface area analysis of both the control and the Biofield Energy Treated silver oxide were performed, and the comparative results are presented in Table 1. The particle size values of the control sample at d_{10}, d_{50}, d_{90}, and D(4,3) were 29.113 µm, 54.856 µm, 94.65 µm, and 58.538 µm, respectively. Similarly, the particle sizes of the Biofield Energy Treated silver oxide at d_{10}, d_{50}, d_{90}, and D(4,3) were 21.339 µm, 43.519 µm, 76.95 µm, and 46.499 µm, respectively. The particle size values in the Biofield Energy Treated silver oxide was significantly decreased at d_{10}, d_{50}, d_{90}, and D (4,3) by 26.70%, 20.67%, 18.7%, and 20.57%, respectively compared to the control sample (Table 1). Therefore, the specific surface area of the Biofield Energy Treated silver oxide (0.176 m^2/g) was significantly increased by 32.33% compared with the control sample (0.133 m^2/g). It can be assumed that the Trivedi Effect®-Consciousness Energy Healing Treatment might act as an external force for reducing the particle sizes of the silver oxide sample, hence increased the surface area. The particle size, shape, and surface area have a significant impact on the solubility, dissolution rate, absorption, bioavailability, and even the therapeutic efficacy of pharmaceutical and nutraceutical compounds [33, 34]. Thus, the Trivedi Effect® Treated silver oxide powder would show enhanced therapeutic properties in pharmaceutical/nutraceutical preparations and would be useful for the industry when it is used as a raw material for the manufacturing.

Powder X-ray Diffraction (PXRD) Analysis

The powder XRD experimental results of both the control and the Biofield Energy Treated silver oxide powder samples showed sharp and intense peaks in the respective diffractograms (Figure 1) which indicated that both the samples were crystalline. The control sample showed the peaks at Bragg's angle (2θ) 18.52°, 20.49°, 26.53°, 32.65°, 33.59°, 37.87°, 39.51°, 54.7°, 65.23°, and 68.5° in the diffractogram (Figure 1). Similarly, the Biofield Energy Treated sample showed the peaks at Bragg's angle (2θ) 18.73°, 20.83°, 26.74°, 32.95°, 33.81°, 37.29°, 39.76°, 54.96°, 65.44°, and 68.79° in the diffractogram (Figure 1). The highest peak intensity showed at 2θ equal to 32.65° in the control and 32.95° of the Biofield Energy Treated sample (Table 2, entry 4). The peak intensities of the Biofield Energy Treated sample were significantly altered compared to the control sample (Table 2). Overall, the peak intensities of the Biofield Energy Treated silver oxide powder were significantly altered in the range from -94.93 to 6.18% compared to the control sample (Table 2). Similarly, the crystallite sizes of the Biofield Energy Treated silver oxide were significantly altered in the range from -54.19% to 54.89% compared to the control sample (Table 2). Overall, the average crystallite size of the Biofield Energy Treated silver oxide powder (398.8 nm) was significantly decreased by 14.66% compared with the control sample (467.3 nm) (Table 2).

The peak intensities and crystallite sizes of the Biofield Energy Treated silver oxide powder sample were significantly altered when compared to the control sample. As per the literature, the peak intensity of any diffraction face on the crystalline compound changes according to the crystal morphology [35], and alterations in the PXRD pattern provide proof of polymorphic transitions [36, 37]. The Biofield Energy Healing Treatment probably produced the new polymorphic form of silver oxide *via* the mediation of neutrino oscillations [10]. Different polymorphic forms of a compound have the significant effects on their physicochemical and thermodynamic properties like melting point, stability, and solubility [38, 39]. Hence,

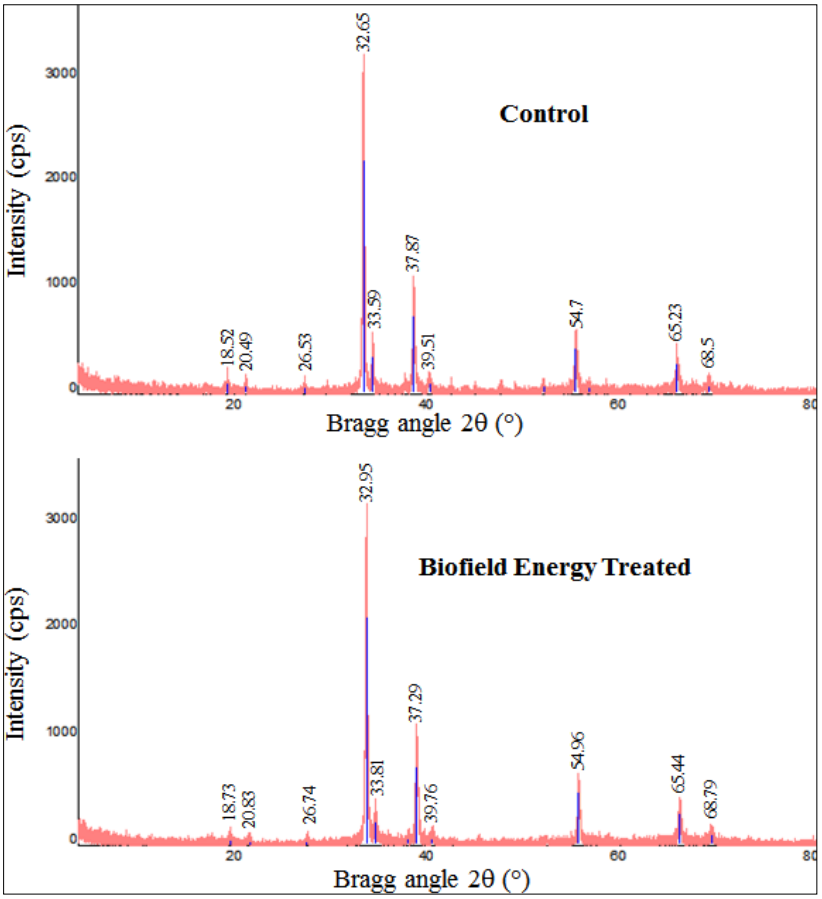

Figure 1. PXRD diffractograms of the control and the Biofield Energy Treated silver oxide.

Table 1. Particle size distribution of the control and the Biofield Energy Treated silver oxide.

Parameter	**d_{10} (µm)**	**d_{50} (µm)**	**d_{90} (µm)**	**D(4,3) (µm)**	**SSA (m^2/g)**
Control	29.113	54.856	94.650	58.538	0.133
Biofield Treated	21.339	43.519	76.950	46.499	0.176
Percent change* (%)	-26.70	-20.67	-18.70	-20.57	32.33

d_{10}, d_{50}, and d_{90}: particle diameter corresponding to 10%, 50%, and 90% of the cumulative distribution, D(4,3): the average mass-volume diameter, and SSA: the specific surface area.
*denotes the percentage change in the Particle size distribution of the Biofield Energy Treated sample with respect to the control sample.

Table 2. PXRD data for the control and the Biofield Energy Treated silver oxide.

Entry No.	Bragg angle (°2θ)		Peak Intensity (%)			Crystallite size (G, nm)		
	Control	Treated	Control	Treated	% change [a]	Control	Treated	% change [b]
1	18.52	18.73	20.00	16.60	-17.00	590.00	353.00	-40.17
2	20.49	20.83	12.10	11.70	-3.31	489.00	224.00	-54.19
3	26.53	26.74	11.20	9.50	-15.18	605.00	436.00	-27.93
4	32.65	32.95	550.00	584.00	6.18	487.00	422.00	-13.35
5	33.59	33.81	91.00	80.00	-12.09	455.00	339.00	-25.49
6	37.87	37.29	205.00	10.40	-94.93	500.00	568.00	13.60
7	39.51	39.76	28.00	22.00	-21.43	273.00	245.00	-10.26
8	54.70	54.96	120.00	127.00	5.83	505.00	521.00	3.17
9	65.23	65.44	87.00	87.00	0.00	503.00	468.00	-6.96
10	68.50	68.79	34.00	29.10	-14.41	266.00	412.00	54.89
11	Average crystallite size					467.30	398.80	-14.66

[a]denotes the percentage change in the peak intensity of the Biofield Energy Treated sample with respect to the control sample.
[b]denotes the percentage change in the crystallite size of the Biofield Energy Treated sample with respect to the control sample.

the Trivedi Effect® Treated silver oxide would be a better option when used to design novel pharmaceutical formulations and also useful for the industry as a raw material for manufacturing.

Differential Scanning Calorimetry (DSC) Analysis

The DSC thermal analysis has been performed and the thermograms of the control and the Biofield Energy Treated silver oxide showed a sharp endothermic peak at 200.7°C and 198.78°C, respectively (Figure 2 and Table 3). The experimental melting point well matches with the reported melting point [1]. The melting point of the Biofield Energy Treated sample was decreased by 0.96% compared with the control sample (Table 3).

The latent heat of fusion (ΔH_{fusion}) of the Biofield Energy Treated sample (4.09 J/g) was significantly decreased by 61.12% compared with the control sample (10.52 J/g) (Table 3). Any change in the molecular chains in the compound structure and any change in the crystal structure in the substance alter the latent heat of fusion [40]. Therefore, it can be presumed that Dahryn Trivedi's Biofield Energy Treatment might have disturbed the molecular chain strength and crystal structure of silver oxide. This could be the possible cause for declining the melting point and latent heat of fusion of the Biofield Energy Treated silver oxide sample compared to the control sample.

Thermal Gravimetric Analysis (TGA) / Differential Thermogravimetric Analysis (DTG)

The TGA thermograms of the control and the Biofield Energy Treated silver oxide samples displayed two steps of thermal degradation (Figure 3). The total weight loss in the Biofield Energy Treated silver oxide (11.32%) was increased significantly by 49.34% compared with the control sample (7.58%). Therefore, the residue amount was 4.05% less in the Biofield Energy Treated silver oxide compared to the control sample (Table 4).

Similarly, the control and the Biofield Energy Treated silver oxide exhibited two peaks (Figure 4) in the DTG thermograms. The maximum thermal degradation temperature (T_{max}) of the 1st peak of the Biofield Energy Treated silver oxide was decreased by 3.07% compared with the control sample. Likewise, the T_{max} of the 2nd peak of the Biofield Energy Treated silver oxide was also decreased by 0.7% compared to the control sample (Table 4). Overall, the thermal stability of the Biofield Energy Treated silver oxide declined compared with the control sample. It can be assumed that Dahryn Trivedi's Biofield Energy Treatment might have disturbed the molecular bond strength of silver oxide, which resulted in the reduction of the thermal stability.

Conclusion

It has been observed that the Trivedi Effect®-Consciousness Energy Healing Treatment has a significant impact on the particle size, surface area, peak intensities, crystallite size, and thermal behaviors of Ag_2O. The particle size values of the Biofield Energy Treated Ag_2O powder were significantly decreased at d_{10}, d_{50}, d_{90}, and D(4,3) by 26.70%, 20.67%, 18.7%, and 20.57%, respectively compared to the control sample. Therefore, the specific surface area of the Biofield Energy Treated Ag_2O powder was significantly increased by 32.33% compared with the control sample. The PXRD analysis of the control and the Biofield Energy Treated Ag_2O powder showed sharp and intense peaks in the diffractograms, indicating that both the samples were crystalline. The peak intensities and crystallite size of the Biofield Energy Treated Ag_2O powder were significantly altered in the range from -94.93 to 6.18% and -54.19% to 54.89%, respectively, compared with the control sample. Overall, the average crystallite size of the Biofield Energy Treated Ag_2O powder was significantly decreased by 14.66% compared with the control sample. The melting point of the Biofield Energy Treated Ag_2O was slightly decreased compared with the control sample. But, the ΔH_{fusion} the treated Ag_2O was significantly decreased by 61.12% compared with the control sample. The total weight loss was significantly increased in the Biofield Energy Treated sample by 49.34% as compared to the control sample. Therefore, the residue amount was 4.05% less in the treated Ag_2O compared to the control sample. The T_{max} of the 1st and 2nd peaks of the Biofield Energy Treated Ag_2O sample were decreased by 3.07% and 0.7%, respectively compared with the control sample. The results suggested that the Trivedi Effect®-Consciousness Energy Healing Treatment might introduce a new polymorphic form of Ag_2O which would show better solubility, dissolution rate, absorption, and bioavailability of Ag_2O

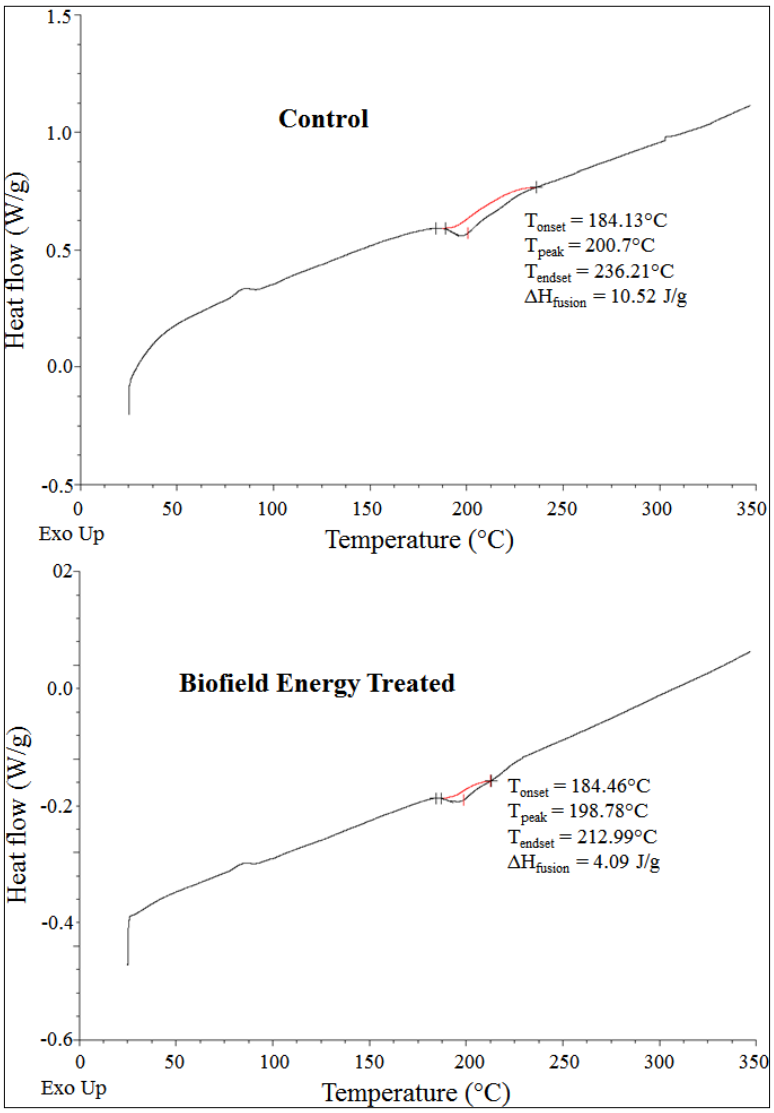

Figure 2. DSC thermograms of the control and the Biofield Energy Treated silver oxide.

Table 3. DSC data for both control and the Biofield Energy Treated samples of silver oxide.

Sample	**Melting point (°C)**	**ΔH (J/g)**
Control Sample	200.70	10.52
Biofield Energy Treated	198.78	4.09
% Change*	-0.96	-61.12

ΔH: Latent heat of fusion,
*denotes the percentage change of the Biofield Energy Treated silver oxide with respect to the control sample.

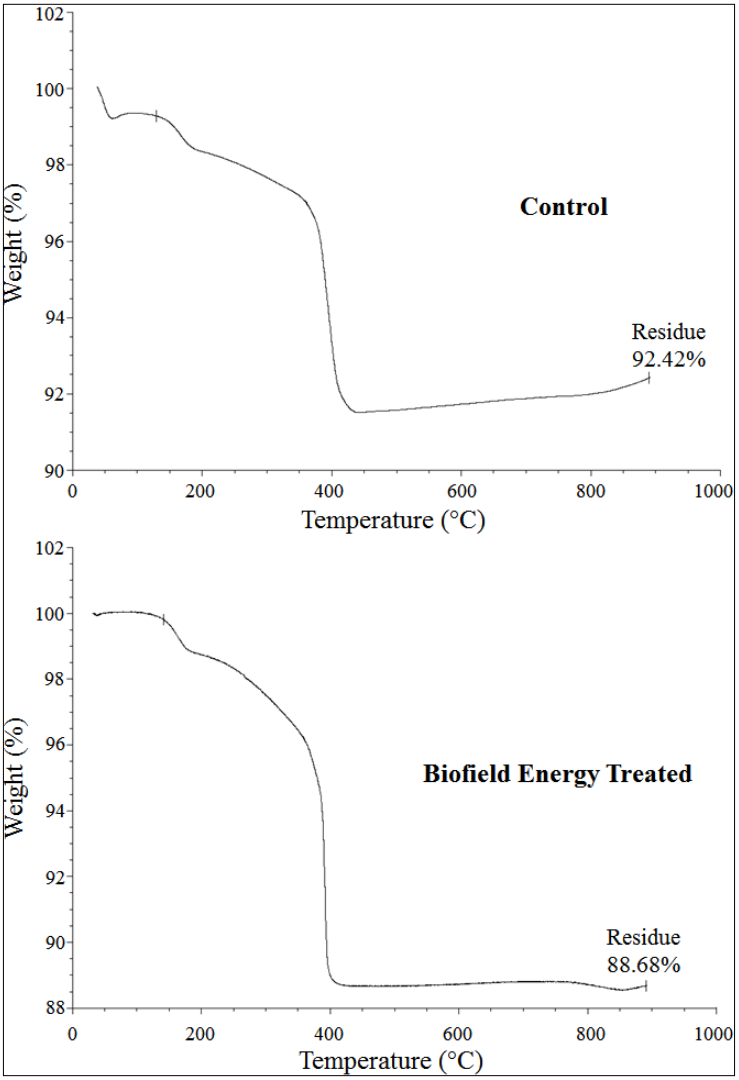

Figure 3. TGA thermograms of the control and the Biofield Energy Treated silver oxide.

Table 4. TGA/DTG data of the control and the Biofield Energy Treated samples of silver oxide.

Sample	TGA		DTG [T_{max} (°C)]	
	Total weight loss (%)	Residue %	1st Peak	2nd Peak
Control	7.58	92.42	168.32	394.58
Biofield Energy Treated	11.32	88.68	163.16	391.8
% Change*	49.34	-4.05	-3.07	-0.70

*denotes the percentage change of the Biofield Energy Treated sample with respect to the control sample,
T_{max} = the temperature at which maximum weight loss takes place in TG or peak temperature in DTG.

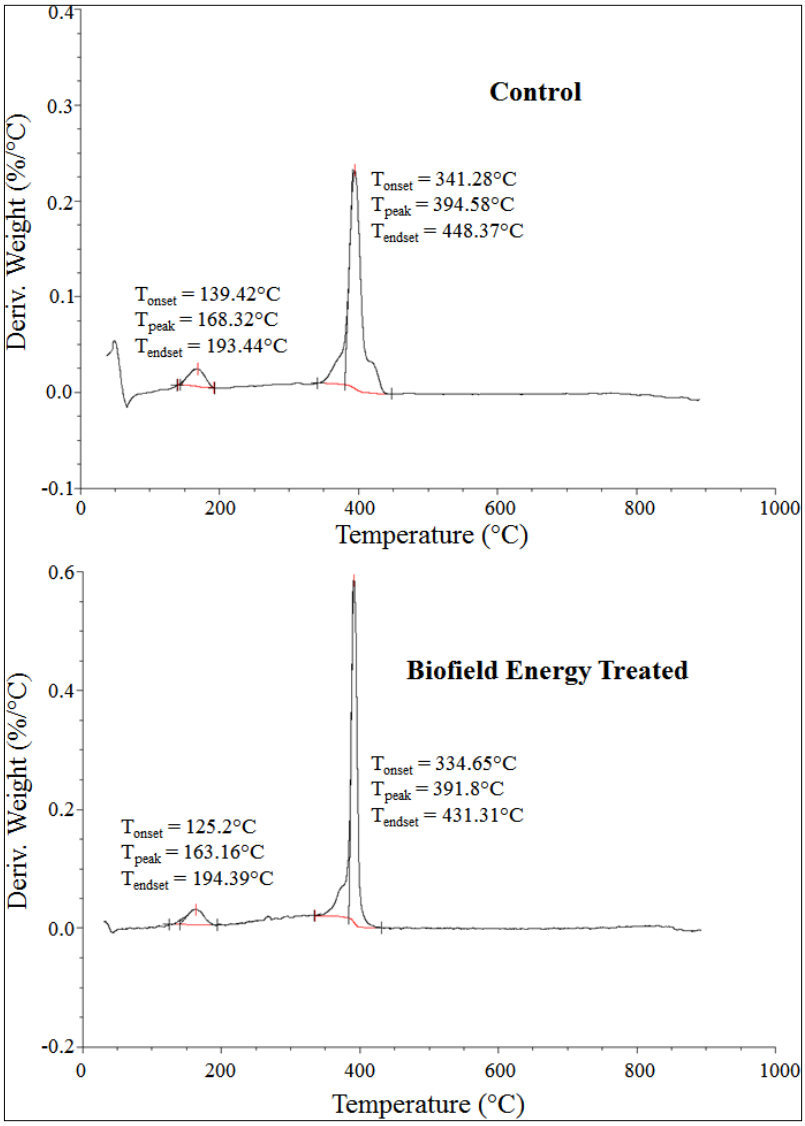

Figure 4. DTG thermograms of the control and the Biofield Energy Treated silver oxide.

in pharmaceutical preparations (i.e., ointments, wound dressing, etc.) and also be advantageous for the many industries (i.e., chemical, space research, nuclear submarines, optoelectronic, etc.) when used as a raw material.

Acknowledgements

The authors are grateful to Central Leather Research Institute, SIPRA Lab. Ltd., Trivedi Science, Trivedi Global, Inc., Trivedi Testimonials, and Trivedi Master Wellness for their assistance and support during this work.

References

1. Allahverdiyev AM, Abamor ES, Bagirova M, Rafailovich M (2011) Antimicrobial effects of TiO_2 and Ag_2O nanoparticles against drug-resistant bacteria and Leishmania parasites. Future Microbiol 6: 933-940.
2. Akiyama T, Miyamoto H, Yonekura Y, Tsukamoto M, Ando Y, et al. (2013) Silver oxide-containing hydroxyapatite coating has *in vivo* antibacterial activity in the rat tibia. J Orthop Res 31:1195-200.
3. https://saltlakemetals.com/msds_silver_oxide/. Retrieved 20-06-2018.
4. Belcaro G, Cesarone MR, Errichi BM, Ricci A, Antelman P, Dugall M, et al. (2011) Silver oxide ointment wound dressing in venous ulcerations:

home, self-management. Panminerva Med 53: 29-33.

5. http://www.creativepen.in/2014/01/uses-of-silver-oxide.html. Retrieved 20-06-2018.
6. Hassan MAM, Agool IR, Raoof LM (2014) Silver oxide nanostructure prepared on porous silicon for optoelectronic application. Applied Nanoscience 4: 429-447.
7. Trivedi MK, Branton A, Trivedi D, Nayak G, Shettigar H, et al. (2015) Antibiogram of multidrug-resistant isolates of *Pseudomonas aeruginosa* after biofield treatment. J Infect Dis Ther 3: 244.
8. Trivedi MK, Branton A, Trivedi D, Nayak G, Sethi KK, et al. (2016) Isotopic abundance ratio analysis of biofield energy treated indole using gas chromatography-mass spectrometry. Science Journal of Chemistry 4: 41-48.
9. Trivedi MK, Mohan R, Branton A, Trivedi D, Nayak G, et al. (2015) Evaluation of biofield energy treatment on physical and thermal characteristics of selenium powder. Journal of Food and Nutrition Sciences. 3: 223-228.
10. Trivedi MK, Mohan TRR (2016) Biofield energy signals, energy transmission and neutrinos. American Journal of Modern Physics 5: 172-176.
11. Rubik B, Muehsam D, Hammerschlag R, Jain S (2015) Biofield science and healing: History, terminology, and concepts. Glob Adv Health Med 4: 8-14.
12. Barnes PM, Bloom B, Nahin RL (2008) Complementary and alternative medicine use among adults and children: United States, 2007. Natl Health Stat Report 12: 1-23.
13. Koithan M (2009) Introducing complementary and alternative therapies. J Nurse Pract 5: 18-20.
14. Trivedi MK, Patil S, Shettigar H, Mondal SC, Jana S (2015) The potential impact of biofield treatment on human brain tumor cells: A time-lapse video microscopy. J Integr Oncol 4: 141.
15. Trivedi MK, Patil S, Shettigar H, Gangwar M, Jana S (2015) *In vitro* evaluation of biofield treatment on cancer biomarkers involved in endometrial and prostate cancer cell lines. J Cancer Sci Ther 7: 253-257.
16. Trivedi MK, Branton A, Trivedi D, Nayak G, Lee AC, et al. (2017) An investigation of the Trivedi Effect®-Energy of Consciousness Healing Treatment to modulate the immunomodulatory effect of herbomineral formulation in male *Sprague Dawley* rats. Advances in Materials 5: 144-153.
17. Branton A, Jana S (2017) The influence of energy of consciousness healing treatment on low bioavailable resveratrol in male *Sprague Dawley* rats. International Journal of Clinical and Developmental Anatomy 3: 9-15.
18. Trivedi MK, Branton A, Trivedi D, Nayak G, Gangwar M, Jana S (2015) Improved susceptibility pattern of antimicrobials using vital energy treatment on *Shigella sonnei*. American Journal of Internal Medicine 3: 231-237.
19. Trivedi MK, Branton A, Trivedi D, Nayak G, Gangwar M, Jana S (2015) Use of energy healing medicine against *Escherichia coli* for antimicrobial susceptibility, biochemical reaction and biotyping. American Journal of Bioscience and Bioengineering 3: 99-105.
20. Trivedi MK, Branton A, Trivedi D, Nayak G, Gangwar M, et al. (2015) Bacterial identification using 16S rDNA gene sequencing and antibiogram analysis on biofield treated *Pseudomonas fluorescens*. Clin Med Biochemistry Open Access 1: 101.
21. Trivedi MK, Branton A, Trivedi D, Nayak G, Bairwa K, et al. (2015) Physical, thermal, and spectroscopic characterization of biofield energy treated murashige and skoog plant cell culture media. Cell Biology 3: 50-57.
22. Trivedi MK, Branton A, Trivedi D, Nayak G, Panda P, et al. (2016) Gas chromatography-mass spectrometric analysis of isotopic abundance of ^{13}C, ^{2}H, and ^{18}O in biofield energy treated p-tertiary butylphenol (PTBP). American Journal of Chemical Engineering 4: 78-86.
23. Trivedi MK, Branton A, Trivedi D, Nayak G, Sethi KK, et al. (2016). Gas chromatography-mass spectrometry based isotopic abundance ratio analysis of biofield energy treated methyl-2-napthylether (Nerolin), American Journal of Physical Chemistry 5: 80-86.

24. Trivedi MK, Branton A, Trivedi D, Nayak G, Gangwar M, et al. (2015) Evaluation of vegetative growth parameters in biofield treated bottle gourd (*Lagenaria siceraria*) and okra (*Abelmoschus esculentus*), International Journal of Nutrition and Food Sciences 4: 688-694.

25. Trivedi MK, Branton A, Trivedi D, Nayak G, Gangwar M, et al. (2015) Morphological and molecular analysis using RAPD in biofield treated sponge and bitter gourd. American Journal of Agriculture and Forestry 3: 264-270.

26. Trivedi MK, Tallapragada RM (2009) Effect of superconsciousness external energy on the atomic, crystalline and powder characteristics of "carbon allotrope powders" Materials Research Innovations 13: 473-480.

27. Trivedi MK, Patil S, Tallapragada RM Effect of biofield treatment on the physical and thermal characteristics of silicon, tin and lead powders J Material Sci Eng 2: 125.

28. Trivedi MK, Sethi KK, Panda P, Jana S (2017) A comprehensive physicochemical, thermal, and spectroscopic characterization of zinc (II) chloride using X-ray diffraction, particle size distribution, differential scanning calorimetry, thermogravimetric analysis/differential thermogravimetric analysis, ultraviolet-visible, and Fourier transform-infrared spectroscopy. International Journal of Pharmaceutical Investigation 7: 33-40.

29. Trivedi MK, Sethi KK, Panda P, Jana S (2017) Physicochemical, thermal and spectroscopic characterization of sodium selenate using XRD, PSD, DSC, TGA/DTG, UV-vis, and FT-IR. Marmara Pharmaceutical Journal 21/2: 311-318.

30. Desktop X-ray Diffractometer "MiniFlex+". The Rigaku Journal 14: 29-36, 1997.

31. Zhang T, Paluch K, Scalabrino G, Frankish N, Healy AM, et al. (2015) Molecular structure studies of (1S,2S)-2-benzyl-2,3-dihydro-2-(1Hinden-2-yl)-1H-inden-1-ol. J Mol Struct 1083: 286-299.

32. Langford JI, Wilson AJC (1978) Scherrer after sixty years: A survey and some new results in the determination of crystallite size. J Appl Cryst 11: 102-113.

33. Khadka P, Ro J, Kim H, Kim I, Kim JT, et al. (2014) Pharmaceutical particle technologies: An approach to improve drug solubility, dissolution and bioavailability. Asian J Pharm Sci 9: 304-316.

34. Buckton G, Beezer AE (1992) The relationship between particle size and solubility. Int J Pharmaceutics 82: R7-R10.

35. Inoue M, Hirasawa I (2013) The relationship between crystal morphology and XRD peak intensity on $CaSO_4.2H_2O$. J Crystal Growth 380: 169-175.

36. Raza K, Kumar P, Ratan S, Malik R, Arora S (2014) Polymorphism: The phenomenon affecting the performance of drugs. SOJ Pharm Pharm Sci 1: 10.

37. Brittain HG (2009) Polymorphism in pharmaceutical solids in Drugs and Pharmaceutical Sciences, volume 192, 2nd Edn, Informa Healthcare USA, Inc., New York.

38. Censi R, Martino PD (2015) Polymorph Impact on the Bioavailability and Stability of Poorly Soluble Drugs. Molecules 20: 18759-18776.

39. Blagden N, de Matas M, Gavan PT, York P (2007) Crystal engineering of active pharmaceutical ingredients to improve solubility and dissolution rates. Adv Drug Deliv Rev 59: 617-630.

40. Zhao Z, Xie M, Li Y, Chen A, Li G, et al. (2015) Formation of curcumin nanoparticles *via* solution-enhanced dispersion by supercritical CO_2. Int J Nanomedicine 10:3171-3181.